THE
AUSTRALIAN
NATIONAL
UNIVERSITY

RESEARCH SCHOOL OF PHYSICAL SCIENCES

ANU-P/704
February 1978

SEMICONDUCTOR X-RAY SPECTROMETERS

A.H.F. Muggleton

Department of Nuclear Physics,
Research School of Physical Sciences,
The Australian National University, Canberra, A.C.T. 2600.

INSTITUTE OF ADVANCED STUDIES

3RD AUSTRALIAN CONFERENCE ON SCIENCE TECHNOLOGY

The Australian National University - 15-17 May 1978

ANU-P/704
February 1978

SEMICONDUCTOR X-RAY SPECTROMETERS

A.H.F. MUGGLETON, C.Eng., M.I.E.R.E., M.Inst.P., M.A.I.P., A.A.I.S.T.

Department of Nuclear Physics,
Research School of Physical Sciences,
The Australian National University, Canberra, A.C.T. 2600.

An outline is given of recent developments in particle and photon induced x-ray fluorescence (XRF) analysis.

Following a brief description of the basic mechanism of semiconductor detector operation a comparison is made between semiconductor detectors, scintillators and gas filled proportional devices.

Detector fabrication and cryostat design are described in more detail and the effects of various device parameters on system performance, such as energy resolution, count rate capability, efficiency, microphony, etc. are discussed.

The main applications of these detectors in x-ray fluorescence analysis, electron microprobe analysis, medical and pollution studies are reviewed.

1. INTRODUCTION

The first semiconductor x-ray spectrometer was described in 1965 by Elad and Nakamura[1], and in 1966 Bowman et al.[2] demonstrated the usefulness of such a system in x-ray fluorescence analysis. Since then improvements in detector design, but mainly in the improvement of associated electronics, has reduced the low energy resolution obtained from 700 eV to less than 105 eV, as reported by Goulding and Stone[3].

Although energy dispersion as a method of analysing x-ray spectra has been known for a considerable time, it has not, until recently, gained widespread acceptance, mainly because, in the past, resolving power of available energy spectrometers has been too poor to separate the x-ray lines from adjacent elements. However, with the improvement obtainable with the semiconductor x-ray spectrometer this disadvantage has mainly disappeared over a large portion of the periodic table.

One of the main advantages of the semiconductor detector system over other types of x-ray spectrometers is the greatly improved resolution over most of the periodic table. The second advantage is speed. These devices are usable at count rates in excess of 10^5 Hz and retain most of their energy resolution capabilities at rates up to 10^4 Hz. The stability of these detectors and their associated electronics is far superior to that obtainable from a proportional counter. Perhaps the most important advantage is the ability to look at the total energy spectrum at one time. Unlike analysis of wavelength dispersion, which is essentially a single channel technique, energy dispersion is a multi-channel technique. With semiconductor detectors, high peak-to-background ratios are achieved and with silicon detectors, escape peak complications in the spectrum are minimised. Finally, properly designed semiconductor spectrometers show none of the count rate dependent gain shrinkage effects observed in proportional counters at high counting rates.

Comparison between the resolution of several types of detector for the ^{55}Fe x-ray spectra is shown in fig. 1; the resolution advantage of the semiconductor device is apparent.

2. PHYSICS OF THE X-RAY FLUORESCENCE METHOD

Every scientist is aware that optical spectroscopy is now a commonplace tool in chemical analysis. However, optical spectra are extremely

complex, caused mostly by the abundance of levels in the outer shells of atoms involved in OPTICAL EMISSION. By observing x-rays, elemental analysis is much more easily achieved, for the inner-atomic-shell structure producing x-rays is relatively simple, and only a few x-ray wavelengths are emitted. X-ray spectroscopy requires both detection of x-rays and measurement of their energy; both functions are performed conveniently by semiconductor detectors.

The simple schematic diagram of a semiconductor x-ray fluorescence spectrometer and the physical mechanisms involved in the fluorescence process are illustrated in fig. 2. Spectroscopy of photo electrons and Auger electrons can also be used for analytical purposes. However, the short range of electrons in materials limits the use of electrons compared with x-ray spectroscopy. A range of methods for exciting characteristic x-rays is available, but the most common technique is to use either a radioactive source or an x-ray tube. Recently an increasing number of workers have been using the proton-induced x-ray technique (PIXE)[4]. The major advantage of PIXE over electron and x-ray excitation is the virtual absence of any low-energy x-ray background. Thus, accurate values for (a) the number of counts under peak, (b) the pulse height of the peak, and (c) the full-width-at-half-maximum (FWHM) can be determined from the "clean" PIXE spectra. The energy of the photon released is characteristic of the atom from which it originates. Therefore if the energy of the exciting radiation is great enough, characteristic x-rays from each atom in the sample are produced. Where an accelerator is available, specific advantages of the charged particle method, such as its potential to analyse very small samples and the ability to selectively analyse surfaces, can be valuable. The ability to scan samples with a fine particle beam is also a very useful analytical feature.

With reference to fig.2, when a photon with energy greater than the K-shell binding energy strikes a K-shell electron, a photoelectric interaction may occur. In such an interaction the energy of the photon is totally absorbed by the electron. The electron is released from the K-shell and travels as a photoelectron with a kinetic energy equal to the energy of the incident photon, minus the binding energy. An electron vacancy is created in the K-shell by the departing photoelectron. This vacancy is filled by an electron from one of the outer electron shells. Since such an electron moves from a higher to a lower energy state, energy is released in the form of characteristic x-rays. These x-rays are released in narrow

bands which correspond to the K-shell binding energy minus the binding energy of the shell from which the replacement electron originated. The K_{α} band predominates and is responsible for about 85% of the characteristic x-rays produced.

The fluorescence yield is the number of x-rays emitted divided by the number of vacancies produced. This is low for elements with low atomic numbers but approaches 100% with middle and high atomic numbers.

Ideally the exciting source should be of high intensity with an energy just above the K-shell absorption edge of the element to be excited.

3. MECHANISM OF OPERATION OF SEMICONDUCTOR DETECTORS

In its simplest analogy, the semiconductor detector can be described as an ionisation chamber in which the gas has been replaced with a solid semiconductor. Fig.3 illustrates how this type of detector operates. The detector consists of two conducting electrodes, the region between being filled with a semiconductor single crystal. A voltage difference is applied across the electrodes, thereby producing an electric field in the semiconductor. A x-ray entering the crystal is totally absorbed and loses its energy by producing free charge carriers, i.e. electron-hole pairs in the semiconductor. These carriers, the number of which is proportional to the energy of the x-ray, move under the influence of the electric field until they are collected at the electrodes or are trapped internally in the crystal. The resulting current represents the basic signal information, the integrated current being proportional to the energy lost by the x-ray. The signal is amplified and shaped to produce a pulse whose amplitude is proportional to the energy lost by the x-ray. This pulse is displayed on the readout of a multichannel analyser.

The advantages of using a solid dielectric are:

a) the high density of the solid results in a much higher efficiency for a given volume
b) more useful geometries are possible
c) smaller dimensions with higher charge carrier mobilities make semiconductors faster than proportional counters (approximately three orders of magnitude faster rise times)
d) most important however is that for a given energy loss, 10 times

more free charge carriers are produced in a semiconductor than in a gas. The ultimate statistical limit on resolution should therefore be better for the semiconductor case. Since the semiconductor crystal is quite stable, most of the short term stability problems associated with gas impurities in proportional counters are absent.

4. THE DETECTOR-CRYOSTAT-PREAMPLIFIER SYSTEM

Semiconductors for x-ray spectrometry are manufactured from either high purity, single crystal, p-type silicon or germanium. The relative merits of these two materials for x-ray detection will be discussed later. Although both silicon and germanium are available in a very pure form, i.e. with electrically active impurities in the order of a few parts per billion, this impurity is still too high to make detectors having a reasonable volume. To compensate these p-type impurities, Pell[5)] developed a technique whereby mobile lithium ions are drifted through the material under carefully controlled conditions of elevated temperature and electric field, thus compensating for the remaining electrically active impurities. An n^{+} - i - p^{+} diode structure is thus formed. The high resistivity intrinsic region, when biased in the reverse mode, is sensitive to x-rays.

Recently high purity single crystal germanium with impurity concentration of less than 5×10^{10} cm^{-3} has become commercially available. The main advantage in using this near intrinsic material is that compensation by lithium drifting is unnecessary. The crystal can therefore be thermally cycled without redistribution of lithium, and precipitation occurring. This advantage is somewhat offset by the cost of the material (twenty times that of the present detector grade germanium). Despite the manufacturing complications associated with lithium drifting, silicon is preferred to germanium, except for very specialised applications, as will be explained later.

The detector structure most commonly used is shown in fig. 4. A trench defines the sensitive volume of the detector and also serves to protect the highly sensitive junction between the i and p regions from contamination. For optimum resolution the detector capacitance must be low; a typical high performance detector has an area of 25 mm^2 and a thickness of 3 mm which keeps the capacitance below 1.5 pF. The detector

entrance window is formed by a gold surface barrier having a thickness equivalent to 0.2 microns of silicon or 1.0 micron of germanium.

In germanium the compensation by lithium is completely unstable at room temperature owing to the high mobility of lithium in the crystal at room temperatures. With silicon devices the storage situation is not so serious and it is possible to allow the silicon device to warm up to room temperature without serious deterioration. However, the lithium compensation in silicon is not completely stable, so it is advisable for long period storage to maintain the device at reduced temperature.

In operation, the detector must be cooled to liquid nitrogen temperature (77°K) to minimise electrical noise caused by thermally excited carriers in the bulk material. The diode is required to operate at liquid nitrogen temperature with a collection field of up to 2000 volts per centimetre, and a leakage current less than 10 pA. As the intrinsic surface of the device is extremely sensitive to atmospheric contamination, efficient cryogenic equipment has been designed to contain the device. Good cryostat design must take into consideration the outgassing of metals and joints used in its manufacture. Other materials used in the system should be chosen for their low outgassing properties. Ideally a stainless steel or aluminium welded construction is preferred with 'O' ring sealed joints kept to a minimum. If ring seals are necessary they should be of indium, copper or some similar material. Soldered joints should be located in the cold part of the cryostat, or have a large surface between them and the detector to act as a vapour trap. Outgassing vapours from soldered joints seem to be a particularly troublesome source of detector surface contamination. Before a cryostat is used it should be thoroughly outgassed and tested for leaks, both at room temperature and liquid nitrogen temperature down to a level of 10^{-10} mℓ/s. The vacuum in the cryostat is maintained using either a molecular sieve in contact with the liquid nitrogen cooled surface or by a small ion pump. A typical detector cryostat assembly is depicted in fig.5. This particular design consists of an internal liquid nitrogen reservoir to the base of which is welded a conducting rod of copper. The semiconductor detector and associated first stage of the preamplifier are mounted on the end of this rod, the whole assembly being surrounded by an evacuated outer housing. The detector bias voltage and the electrical signal pulses generated in the detector are transferred through hermetically sealed electrodes in the cryostat wall. After the cryostat has been evacuated

via the pumpout/pressure relief valve, the vacuum is maintained by means of the molecular sieve, as illustrated. The molecular sieve consists of metal alumina silicates in granular form. When the sieve is cooled to liquid nitrogen temperature it has the characteristic of absorbing many times its own volume of gas. Providing the sieve material is maintained at cryogenic temperatures the absorbed gases will be retained indefinitely. The vacuum not only keeps the detector clean, it also acts as thermal insulation to prevent excessive "boil-off" of liquid nitrogen. The inter-space between inner reservoir and outer casing is filled with a super insulating material, such as thin aluminised Mylar foil, to further reduce liquid nitrogen consumption. Typical "boil-off" rates for such an assembly are less than 0.5 litre of liquid nitrogen per day. As the molecular sieve has the ability to absorb many times its own volume of gas at liquid nitrogen temperature, in the unlikely event of a small vacuum leak developing and the reservoir being allowed to run out of liquid nitrogen, sufficient internal gas pressure could build up to constitute an explosive hazard. A pressure release valve is incorporated which automatically operates when the internal pressure exceeds 1.5 atmospheres. The cryostat entrance window is made from 0.0003" beryllium which gives good x-ray transmission down to 1.0 keV (fig.6).

The detector itself is housed in an aluminium mount and insulated from earth potential by either sapphire, beryllia or boron nitride rods. The collection voltage is applied to the p^+ side of the diode, the n^+ side being light-coupled to the first stage of the charge sensitive preamplifier, which comprises a specially selected field effect transistor (FET).

The resistor, traditionally used to provide low-frequency feedback to a low-noise preamplifier is replaced by light coupling from a light-emitting diode (LED) to the photosensitive drain-gate FET junction. This step eliminates the feedback resistor, a noisy and unreliable component; it also entails remounting the small FET silicon chip in a new package, thereby eliminating noise produced by the FET header. The elimination of these noise sources permits use of longer pulse-shaping times in the main amplifier, thereby achieving energy resolutions below 100 eV at low counting rates. In a simple light-feedback system, non-linearity of the LED current-light relationship causes degradation of performance at higher counting rates. Therefore the majority of present day systems use a pulsed-light feedback assembly whereby the LED is pulsed when necessary to maintain the preamplifier

output in its normal range. When pulsing occurs, a reject waveform is fed to the main amplifier, and all signals are rejected until the system resumes normal operation.

The FET exhibits its minimum noise level at a temperature in the region of 100°K (approximately 23°K higher than liquid nitrogen temperature). A zener diode is used to heat the FET and maintain it within the optimum temperature range.

A drawing of the relative location of the remounted FET, light diode and zener diode within the cryostat is shown in fig. 7. Care is taken to keep critical leads short and rigid to reduce microphonics.

5. MICROPHONICS

One of the most serious problems with very low noise systems is their sensitivity to microphonics. Microphonic noise generation can be a serious source of resolution broadening. In cryogenic systems, mechanical vibrations of the input circuit components with respect to surfaces at different potentials are induced by bubbling of liquid nitrogen, turbulence from automatic nitrogen transfer systems, vibration of other equipment in contact with the detector cryostat, and environmental noise.

To generate a microphonic signal with the amplitude of 10 eV (Si), a change of capacitance between the FET gate and the high voltage (detector bias 1000 V) of only 5×10^{-7} pF is required, Elad[6]. Since the typical stray capacitances are of the order of 1 pF, relative mechanical motions (within the frequency pass-band of the shaping amplifier) of approximately 10^{-7} are significant. Since most of the vibration problems are relatively low frequency, much of the microphonic noise is filtered out by the limited amplifier pass-band. Consequently, microphonic problems are usually more serious at long shaping time constants. The design of the detector and preamplifier package is critical. FET gate to detector connection should be a minimum length and all wiring should be securely tied down. It is imperative that the h.t. lead is shielded from the FET and that internal wiring is so arranged to eliminate any possibility of earth loops. The detector/preamplifier package is normally surrounded by an aluminium shield thermally connected to the cryostat cold finger. The purpose of this shield is threefold: (a) to reduce microphony, (b) to act as a contamination shield, and (c) to reduce "black body" infra-red radiation from the cryostat

walls which will raise the temperature of the detector and consequently increase the leakage current.

6. DETECTOR NOISE

Both leakage current in the detector and detector capacitance contribute to system noise and resolution degradation. At the present state-of-the-art, detector leakage current can be a negligible factor for detectors cooled to liquid nitrogen temperature (77°K). However, since detector noise increases more rapidly with rising temperature than does FET noise, detector noise can be expected to become a major contribution at temperatures above 200°K.

7. CHARGE LOSSES

Loss of free charge carriers, because of trapping throughout the semiconductor crystal, can be a significant source of spectral distortion. The peak width broadening from this effect increases with increasing energy of the x-ray and will be more pronounced at higher energies. This problem, which is often a function of detector bias voltage, frequently results in low energy tails on monoenergetic spectral lines, and is therefore often more readily quantified by changes in the full width tenth maximum (FWTM) than the full width half maximum (FWHM) of the spectral peak.

Windows and dead layers, which are not intimate parts of the detector element, cause a loss of efficiency at low x-ray energies. Charge loss in "partially-dead" layers (Walter [7]) in the detector adjacent to the entrance window can result in both a loss of full energy peak efficiency and in undesirable spectral distortion in the form of low energy tails, ghost peaks and non-linearities.

8. ENERGY RESOLUTION

In practice the energy resolution of a detector is specified as the full width at half maximum (FWHM) of a spectral peak. This quantity can be expressed as a percentage of the incident energy but is more usually specified in terms of energy measured in electron volts.

The most fundamental factor affecting the resolution of semiconductor

spectrometers is line broadening due to the statistical uncertainty involved in converting the incoming incident energy into free charge carriers. For true Poisson or true random statistics in the energy loss mechanism (energy conversion to free charge process), the statistical broadening of the monoenergetic energy peaks can be easily calculated. Assuming a gaussian line shape, by Poisson statistics the FWHM of the peak should be $2.35(wE)^{1/2}$, where E is the energy of the incident radiation and w the factor relating the energy to the number of free carriers created, i.e. $N = E/w$.

In fact this process does not follow Poisson statistics because the multiple events that occur in the energy loss process are correlated; the form of the statistical formula must therefore be modified. This is done by inserting a correction factor F called the Fans factor, (Fano[8]), such that:

$$\Delta E \text{ FWHM} = F^{1/2}\left\{8(\ln 2)wE\right\}^{1/2} = 2.35(FwE)^{1/2}. \qquad \text{(Eqn. 1)}$$

This corrects for the fact that the real broadening is not as bad as predicted by Poisson statistics. The Fano factor is less than unity, and for silicon and germanium is thought to be 0.087 ± 0.03 and 0.053 ± 0.02 respectively (Zulliger and Aitkin[9]).

It can be seen simply by looking at the equation for statistical broadening (eqn. 1) that semiconductors have an advantage over the scintillator or proportional counter. It takes almost ten times as much energy to create a free charge carrier in a gas therefore only one tenth as many charge carriers are created. The semiconductor detector therefore has better resolution capabilities than either the scintillator or gas-filled proportional counter. According to the square-root relationship, this would mean about three times the statistical broadening.

The factors limiting resolution may be listed under the headings: (i) statistical fluctuations in the ionization process; (ii) incomplete charge collection; (iii) "window" effects of the surface; (iv) electrical noise arising in the counter; (v) noise arising in the electronic circuitry. The overall resolution of a detector is the square-root of the sums of the squares of all these contributions. In practice (i), (ii) and (iii) are usually fairly small and (iv) can be controlled by keeping the detector capacitance small and by ensuring the field and surface leakages are not excessive.

Over the past few years resolutions have gradually improved as better semiconductor crystals became available. The main improvement however has been in the field of low noise electronics. Currently the design of detector and electronics for x-ray fluorescence spectrometers has reached a fairly stable state and significant changes cannot be expected for the next few years (Goulding[10]).

9. COMPARISON BETWEEN SILICON AND GERMANIUM DETECTORS

Because the ionization potential of germanium is less than that of silicon one would expect germanium detectors to give a resolution slightly superior to that of silicon detectors. However, until the Fano Factors for both germanium and silicon have been finally determined it is not possible to decide which material gives intrinsically better resolution.

The photopeak efficiency of silicon and germanium detectors for 2 to 100 keV photons can be calculated from their mass attenuation coefficients. At energies below 4 keV the detector efficiency is determined by the thickness of the beryllium window. Fig.8 shows the variation in efficiency with incident photon energy of typical (3 mm and 5 mm thick) germanium and silicon detectors with 0.010, 0.005, 0.002 and 0.001" thick beryllium windows. Fig. 6 shows the percentage absorption for a range of beryllium window thickness. From the graph it is evident that germanium should be used for energies above 20 keV.

Germanium has the disadvantage that it must be constantly maintained at a low temperature because of high lithium ion mobility in the crystal lattice. If a germanium detector is allowed to reach room temperature the result can be catastrophic with the consequent loss of the detector.

A further disadvantage of germanium compared with silicon is the presence of relatively large escape peaks with the former. These escape peaks undoubtedly complicate the interpretation of x-ray spectra and sometimes result in silicon being preferred to germanium, even in the detection of photons at high energies.

10. APPLICATIONS OF SEMICONDUCTOR X-RAY SPECTROMETERS

For qualitative analysis the semiconductor x-ray spectrometer is

rapid, has high resolving power and can display the whole elemental spectrum at one time. The lower limit of elemental detection is set by the thickness of the beryllium entrance window of the cryostat. Fig.9 shows the state-of-the-art resolution obtained with a window-less system using 350 keV proton excitation.

However, quantitative analysis is more complex as corrections have to be made for fluorescence yield (which is different for each element), atomic number, absorption, and matrix effects, and background subtractions. For absolute quantitative analysis a small computer can be used either in place of, or in conjunction with, the multichannel analyser. However, for repetitive analysis it is sufficient to compare the results with a known standard.

Semiconductor x-ray spectrometers are distinguished by their ability to survey simultaneously a whole spectrum of trace elements present in levels less than 1 ppm (Goulding[11]). More sensitive methods can be devised for particular elements, e.g. atomic absorption for such elements as mercury but extensive sample preparation is required. Neutron activation can exhibit greater sensitivity than x-ray fluorescence for some elements, but for others its sensitivity is poor, and the activation process is slow and costly. It thus becomes apparent the x-ray fluorescence analysis will find an ever growing range of applications.

A partial listing of the many diverse fields of interest for which the semiconductor non-dispersive x-ray spectrometer has generated widespread interest is summarised in table 1 together with some representative applications[7].

10.1 Electron Column Devices

Semiconductor spectrometers are being used extensively with both Electronprobe Microanalysers and Scanning Electron Microscopes. The advantage of simultaneous multi-element analysers and the absence of spurious ghost peaks makes it possible for the spectrometer to locate quickly the elements present in areas of interest on a sample before detailed analysis with the microprobe. Semiconductor spectrometers can easily be attached to existing parts of the microprobe. The lower energy limit of the system is determined by the cryostat beryllium window. However,

TABLE 1

Fields of interest for which the semiconductor non-dispersive x-ray spectrometer may be used.

Field of Interest	Typical Examples
Nuclear physics	Coster-Kronig transition probabilities[12]; K and L subshell transition probabilities[13].
Medicine and biochemical research	Examination of tissue specimens, cells, etc., in electron microprobe or scanning electron microscope (SEM); analysis of trace elements in blood and glands by fluorescence analysis; non-radioactive iodine uptake; analysis of clinical x-ray sources.
Metallurgy	Analysis of grain boundaries, diffusion profiles etc., in electron microprobe and SEM; qualitative and semi-quantitative analysis of alloys by fluorescence analysis; studies of lattice spacing in high pressure, high temperature phase transitions and other transient phenomena by x-ray spectrography.
Geophysical research and resource exploration	Ocean-bottom core analysis; classification of mineral samples; mineral and precious metal exploration.
Solid state and semiconductor research and development	Analysis of semiconductor device failure modes using the electron microprobe and SEM; studies of spatial distribution of impurities in devices and materials.
Space exploration	X-ray astronomy (efforts to identify characteristic lines in the x-ray continuum); classification of minerals, etc., from Apollo lunar samples; analysis of samples from meteors, asteroids, and the planets[14].
Forensic science	Identifying art and coin forgeries; customs control of suspected precious metals, etc.; identification of heavy element poisons; validation of passports, etc.
Industrial	Analytical laboratory quality control and failure analysis; on-line process control for steel mills, metal refining[15], etc., engine wear monitoring by fluorescence analysis of the lubricating oil; thickness gauging; identifying and sorting unknown metal samples.
Environment analysis and public safety	Trace analysis for toxic heavy elements including field analysis for toxi lead paint concentrates, from gasoline; fluorescent analysis of environmental pollutants and air filter samples[11].
Archaeology and art	Authentication and classification of archaeological artifacts, dating, geographical origin, etc.; identification and authentication of old paintings, coins, etc.

since the microprobe also operates under vacuum, it is possible to reduce the window thickness considerably or even work without one in a ultra-high vacuum system. Such ins. uments are now co mercially available.

The Scanning Electron Microscope (SEM) is similar to the electron probe microanalyser since both instruments use electromagnetic lenses to demagnify the beam from a high voltage (20 to 50 kV) electron gun into a fine probe which may be scanned over the sample surface in a raster pattern. The major basic difference in these two instruments results from the fact that the microprobe has a beam spot diameter of 1 to 0.2 µm while the SEM beam is typically less than 200 Å in diameter. In order to achieve this improvement in spatial resolution, it is necessary to reduce the beam current by about four orders of magnitude. The resultant reduction in x-ray intensity makes use of wavelength dispersion analysis on the SEM difficult and in many cases impractical. Measurement of the characteristic x-ray excited by the electrons is the only unambiguous source of qualitative and quantitative information about the elemental constituents of the sample. Thus, although the energy dispersing spectrometer may be classed as a very useful accessory for probe microanalysers, it must be considered as essential to a well equipped SEM. Fig.10 shows the topographical and element mapping of a Sugarbeet leaf and a Rice leaf respectively, using an x-ray spectrometer in conjunction with a SEM. The distribution and location of the elements of interest, i.e. Si and Br, are clearly depicted.

10.2 Pollution Studies

Particulate deposits on air pollution filters present a simple problem for the XRF technique. With short sample collection times, the mass of the particulate deposit becomes a substantial fraction of the air-filter material. Consequently, background due to backscatter in the filter material is small. Fig.11 shows a typical filter sample collected over Sydney.

10.3 Trace Elements in Body Fluids

By utilizing a detector geometry employing a guard ring construction to reduce background, and using an x-ray tube to excite the element under investigation, Goulding[11] has detected very low levels of lead in blood. With a 3 mℓ sample, 0.25 ppm of Pb were detected in a counting time of 15

minutes. Other elements such as iron and iodine should be readily detectable (fig. 12).

10.4 Miscellaneous Applications

Semiconductor spectrometers are being used to investigate the composition of museum pieces, objects of art and pigments used in paintings to help in deciding on manufacturing technique, authenticity, etc. (fig.12).

11. CONCLUSIONS

The use of semiconductor XRF analysis continues to grow in popularity. Although other analytical techniques possess specific features such as sensitivity, specificity, wide elemental coverage, low cost, etc. which make them superior in certain circumstances, few methods have the versatility of x-ray fluorescence. Its ability to determine rapidly and non-destructively most trace elements in solids and liquids with little sample preparation has led to its widespread adoption for a great variety of analytical requirements.

REFERENCES

1. E. Elad and K. Nakamura, Nucl.Instr. & Meth. 42 (1966) 315.

2. H.R. Bowman, E.K. Hyde, J.E. Thompson and R.D. Jarad, Science 151 (1966) 562.

3. F.S. Goulding and Y. Stone, University of California Research Laboratories Report UCRL-19860 (1970).

4. Proceedings of the International Conference on Particle Induced X-ray Emission and its Analytical Applications, Lund, Sweden, August 1976. Nucl.Instr. & Meth. 142 (1977).

5. E.M. Pell, J.Appl.Phys. 31 (1960) 291.

6. E. Elad, Proc. ASTM Workshop "Energy dispersion x-ray analysis" (Toronto, June 1960).

7. F.J. Walter, IEEE Trans.Nucl.Sci., NS-17, No.3 (1970) 196.

8. U. Fano, Phys.Rev. 72 (1947) 26.

9. H.R. Zulliger and D.W. Aitken, IEEE Trans.Nucl.Sci. NS-17, No.3 (1970) 187.

10. F.S. Goulding, Nucl.Instr. & Meth. 142 (1977) 213.

11. F.S. Goulding and J.M. Jaklevic, University of California Research Laboratories Report UCRL-206.5 (1971).

12. R.E. Wood, Phys.Rev. 187 (1969) 1497.

13. A. Karttunen, Nucl.Phys. A131 (1969) 343.

14. H. Alfren and G. Arrhenuis, Science 167 (19.0) 139.

15. A.P. Langheinrich and J.W. Forester, Advan. X-Ray Anal. 11 (1968) 275.

16. D.A. Landis et al. Nucl.Instr. & Meth. 101 (1972) 127.

17. D.A. Landis et al. Nucl.Inst. & Meth. 87 (1970) 211.

18. R. Woldseth, X-Ray Energy Spectrometry, Kevex Corp., Foster City, California 94404.

FIGURE CAPTIONS

FIG. 1. Resolution comparison between scintillation, proportional and semiconductor Si(Li) detectors [Woldseth, R.[18]].

FIG. 2. Basic x-ray fluorescence spectrometer and the atomic process.

FIG. 3. Operation of a semiconductor radiation detector.

FIG. 4. Configuration of a standard Si(Li) detector, cutaway view [Woldseth, R.[18]].

FIG. 5. Detector/cryostat assembly.

FIG. 6. Transmission-energy curves for thin beryllium windows.

FIG. 7. Drawing of a cryostat showing FET assembly and detector [Landis[16]].

FIG. 8. Efficiency of Si and Ge x-ray detectors.

FIG. 9. Spectrum of carbon fluoresced with 350 keV protons [Woldseth, R.[18]].

FIG. 10. Topographical and element mapping with SEM.
1. Sugar beet leaf (A) Secondary electron image; (B) Br x-ray map; (C) Overlap of (a) and (B).
2. Rice leaf (D) Secondary electron image; (E) Silicon x-ray map; (F) Overlap of (D) and (E) [Woldseth, R.[18]].

FIG.11. IXA analysis of sample of particulate matter collected from Sydney air.

FIG.12. (a) Fluorescence x-ray spectrum obtained on a blood serum specimen using a spectrometer equipped with guard-ring detector and reject circuitry. (b) Spectrum obtained on the same sample with the same geometry, and the same total counts in the scatter peak, but with a simple top-hat detector [Landis[17]].

FIG.13. Determination of the authenticity of a bronze Greek statuette by using a semiconductor x-ray spectrometer; (a) Alleged ancient bronze; (b) Genuine ancient bronze; (c) Modern bronze. [By kind permission of the National Museum of Antiquities of Scotland].

Fe^{55} X-RAY SPECTRA

——— 1/32" NaI(Tl) ON EMI 9656 R
—·— TYPICAL PROPORTIONAL COUNTER
— — — REALISTICALLY ATTAINABLE WITH SMALL Si(Li)

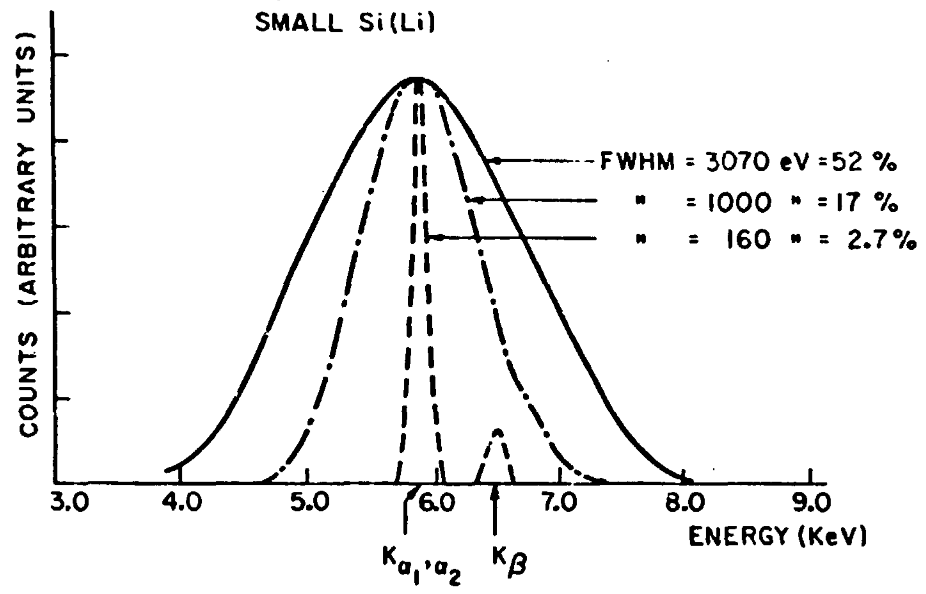

FIG. 1

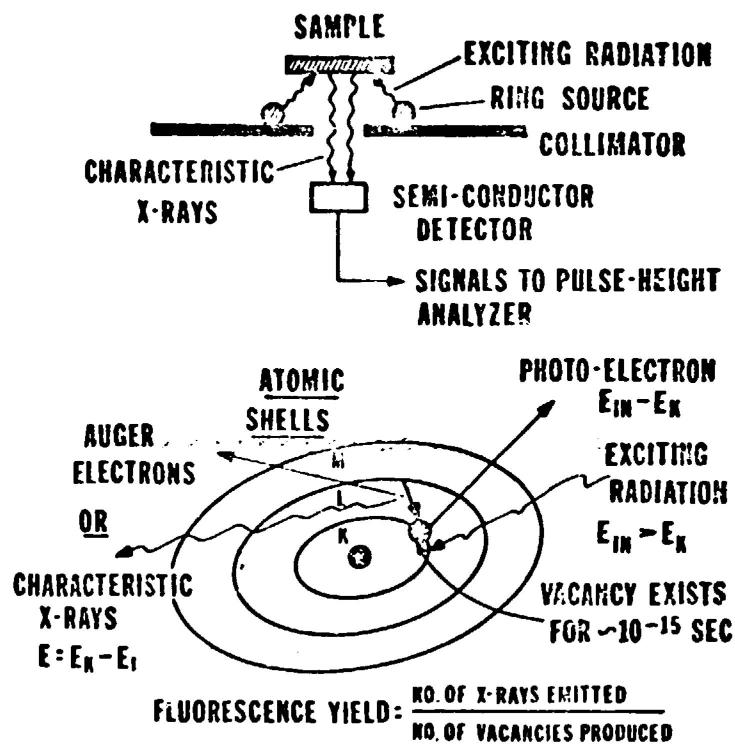

FIG. 2

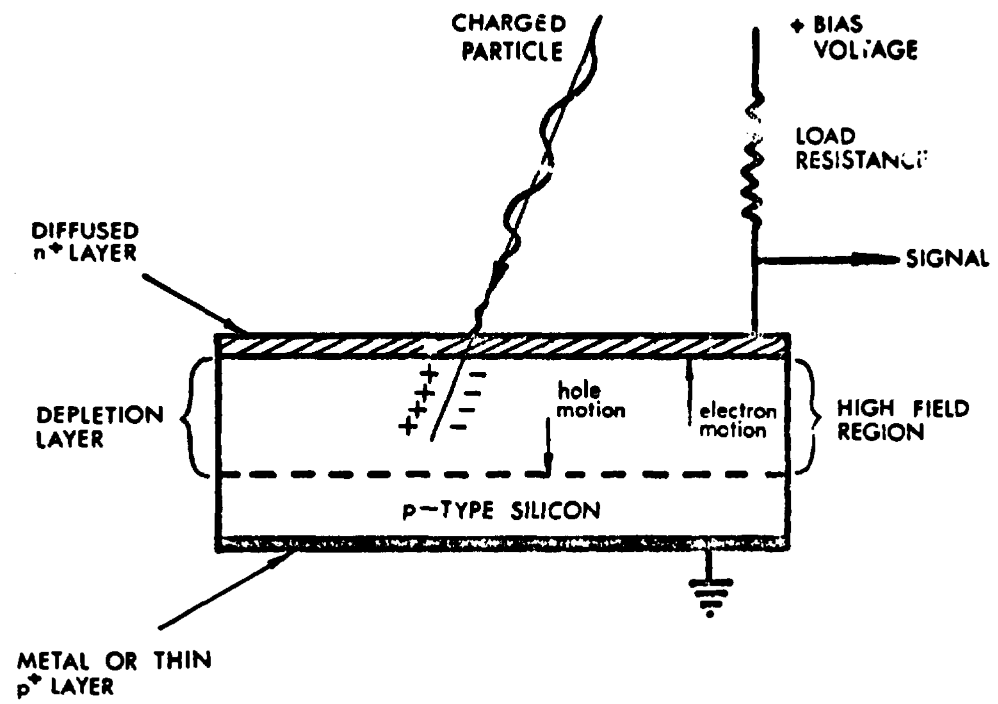

FIG. 3

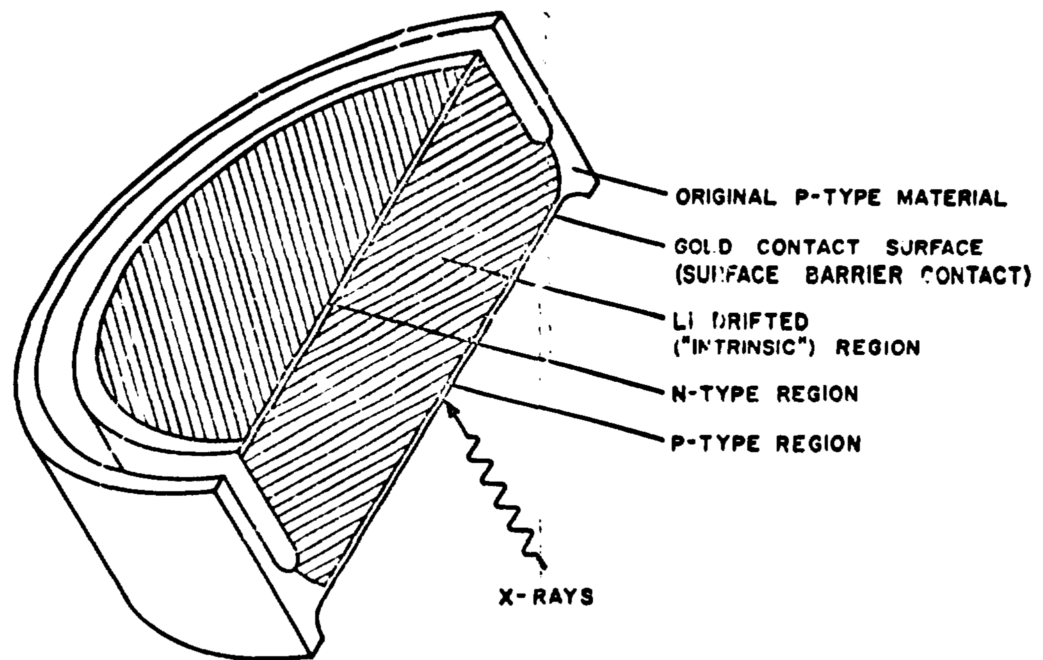

FIG. 4

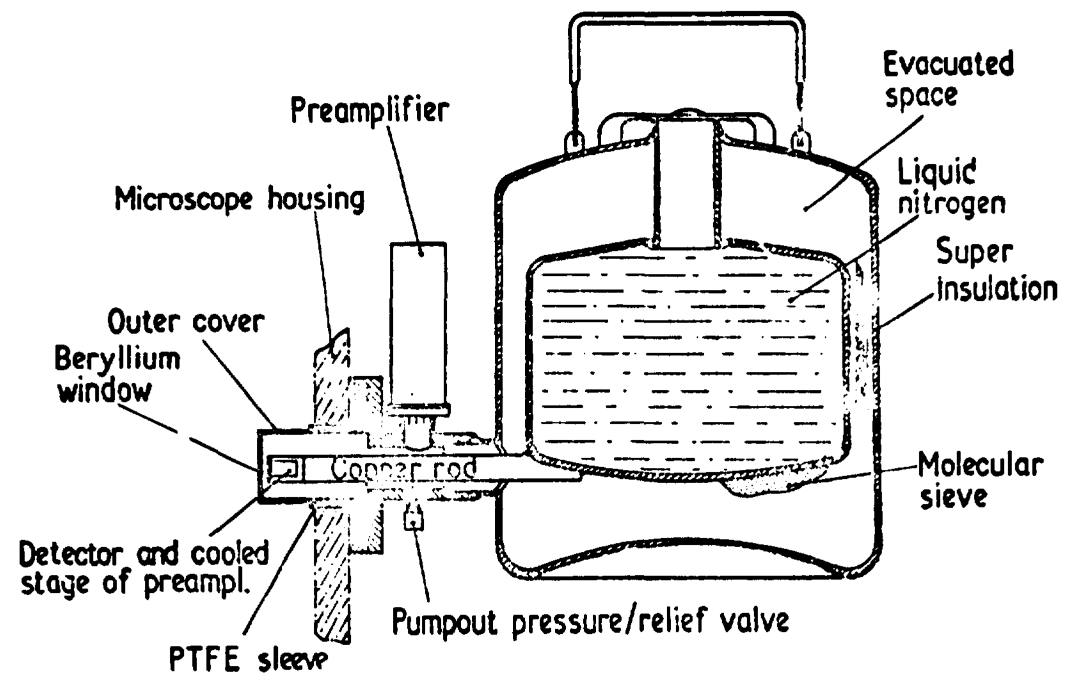

FIG. 5

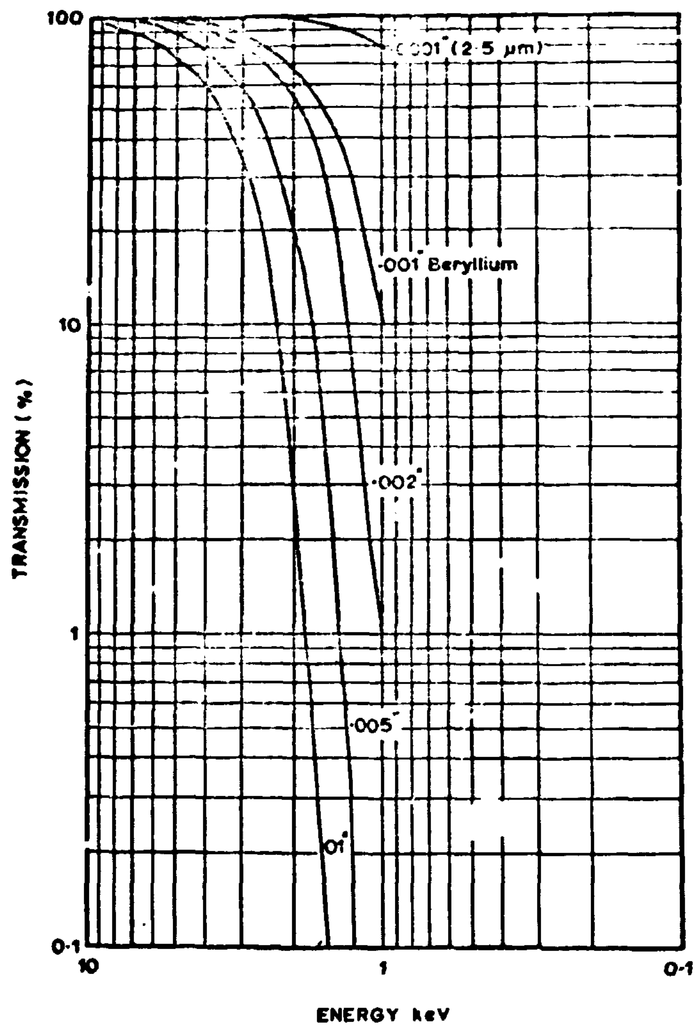

FIG. 6

FIG. 7

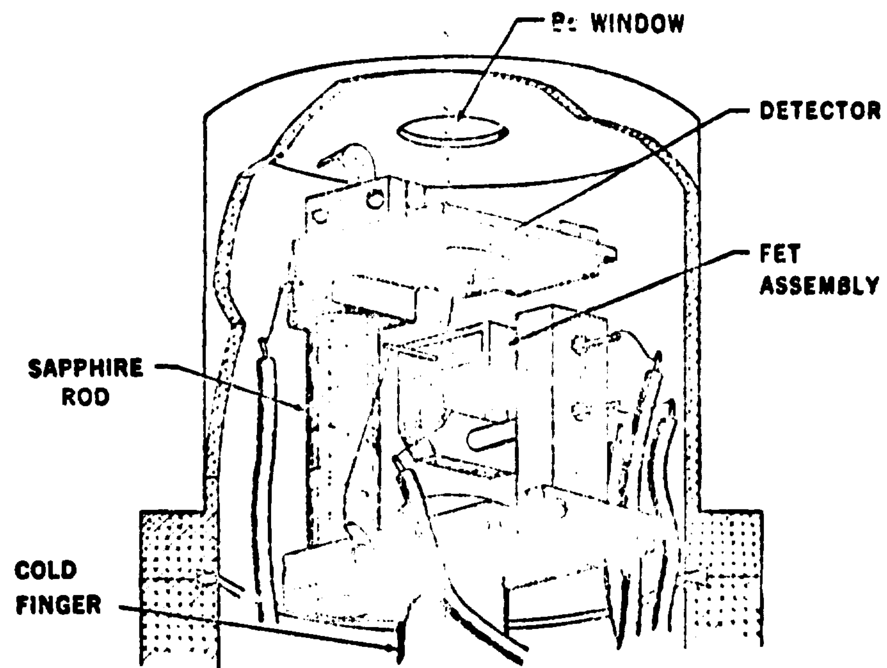

Fig. 5. Drawing of cryostat showing FET assembly and detector.

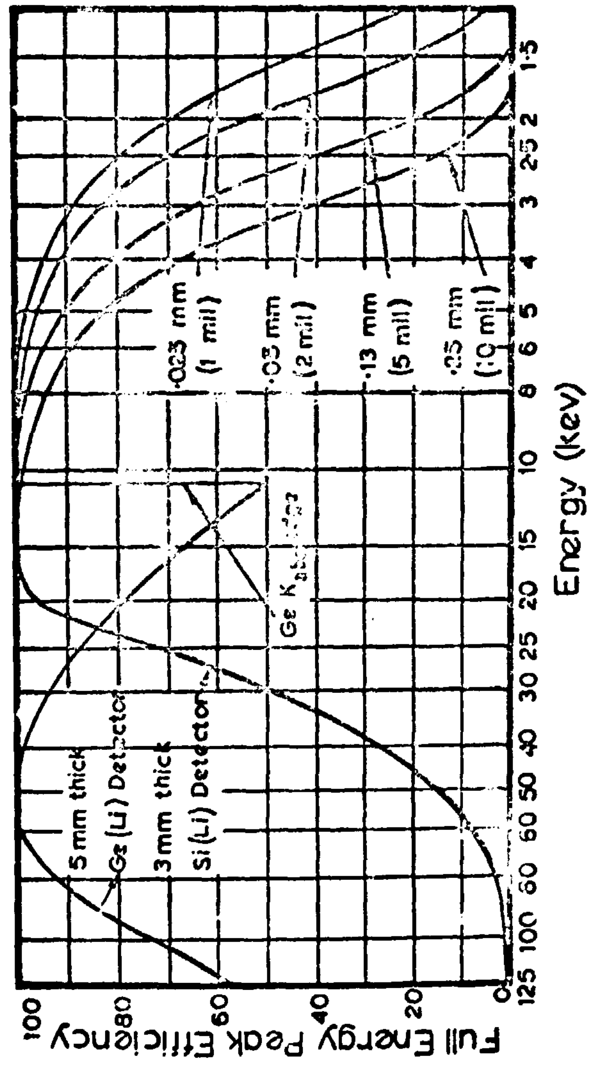

FIG. 8

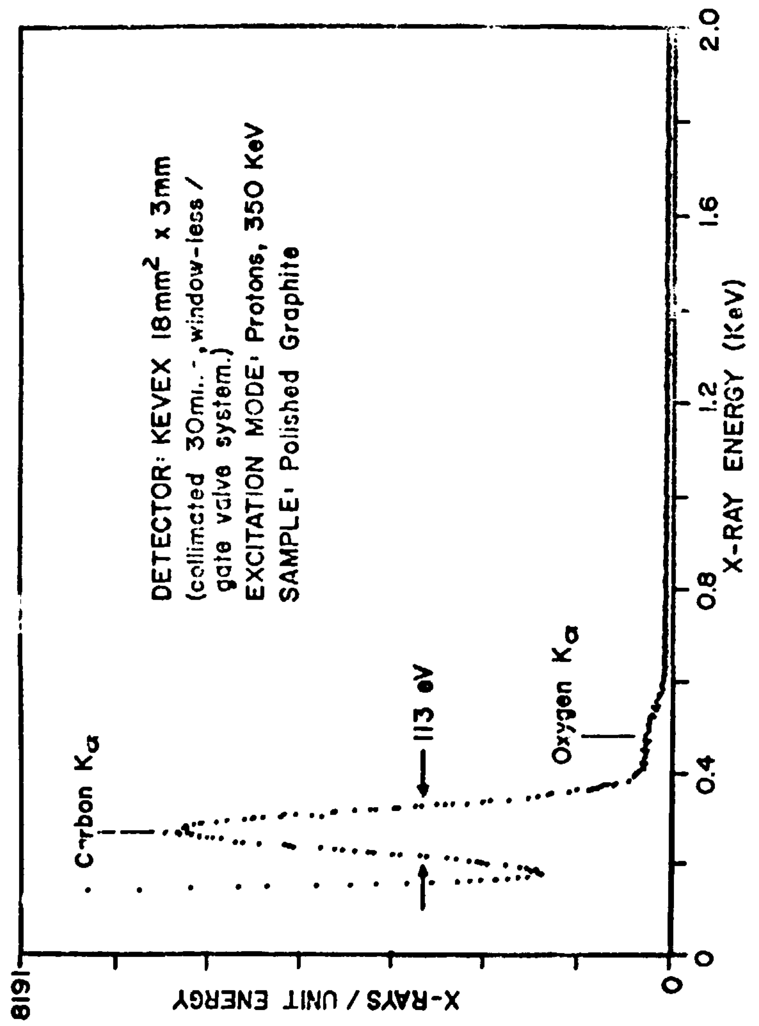

FIG. 9

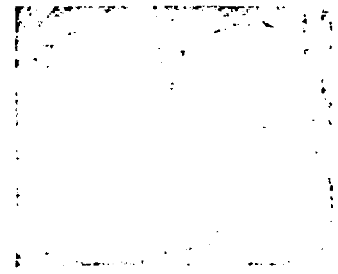

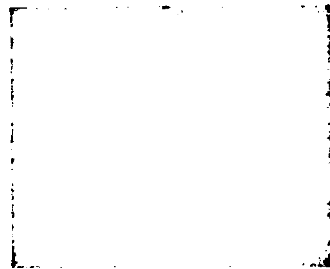

(c)

FIG. 10

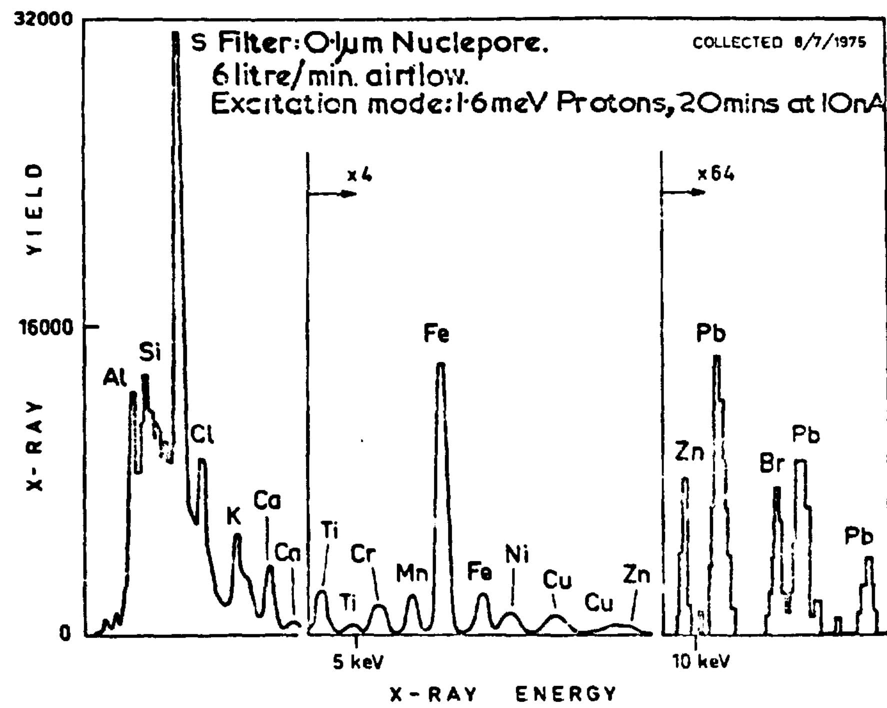

FIG. 11

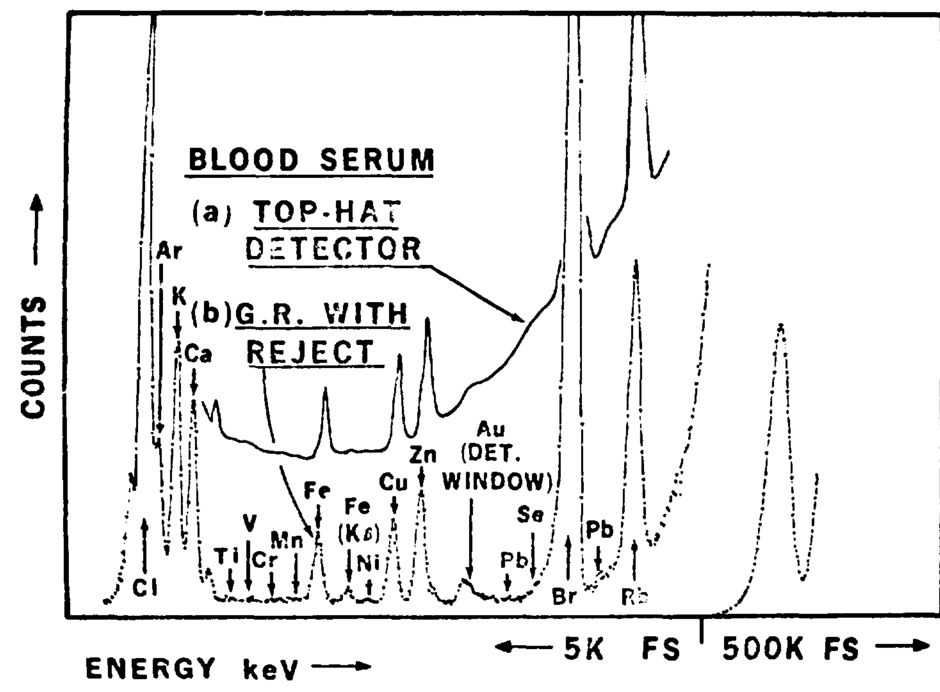

FIG. 12

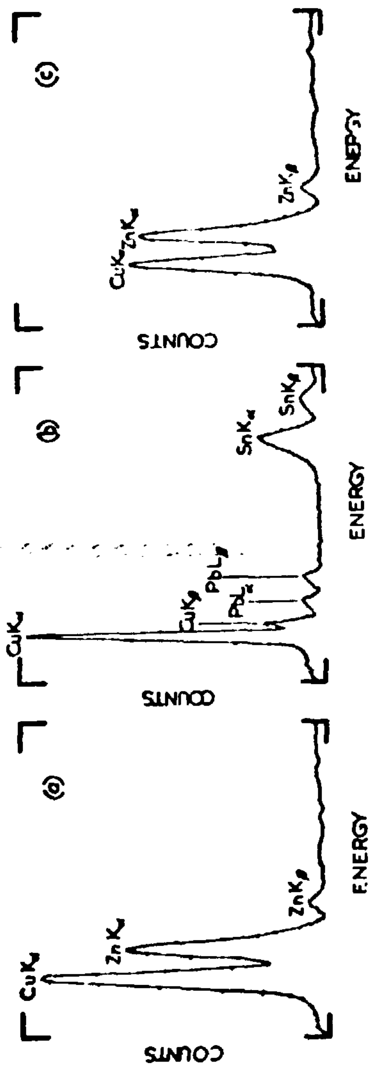

FIG. 13